

C. Snyder<sup>1</sup> and D. Keyser<sup>2</sup><sup>1</sup>National Center for Atmospheric Research\*, Boulder, Colorado, USA<sup>2</sup>State University of New York at Albany, Albany, New York, USA

## 1. INTRODUCTION

Observations, numerical simulations, and intuition all suggest that the planetary boundary layer (PBL) strongly modifies surface fronts. Indeed, many surface fronts, even those that are largely cloud free and nonprecipitating, exhibit density-current-like structure at their leading edges. Because of the variety of physical processes in the PBL, and given the dearth of knowledge of how these processes modify fronts, we consider idealized two-dimensional (2D) fronts with PBL physics restricted to surface drag and parameterized turbulent mixing; neither surface heat flux nor moist processes are included. In particular, we ask: (1) Do surface drag and its associated turbulent mixing produce net frontogenesis or net frontolysis? (2) What is the structure of the resulting surface front and how is it related to a density current?

## 2. IS SURFACE DRAG FRONTOGENETIC?

The answer to the above question depends on the strength of the front, as this determines the dynamics of the frictionally driven flow in the PBL.

For broad fronts with small temperature gradients, advective terms will be small and the PBL typically will be characterized by a balance between Coriolis force, pressure gradient, and divergence of turbulent stress. The dynamics of the flow are then quasi-geostrophic in the interior coupled to an Ekman layer at the surface (generalized to include surface drag and variable eddy viscosity  $K$ ).

An example is “frontal spin-down,” i.e., the evolution of a 2D baroclinic zone subject to Ekman pumping at  $z = 0$ . A suitable quasi-geostrophic solution is

$$\theta = \frac{\Delta\theta}{\pi} \tan^{-1} \left( \frac{x/L}{1 + z/H + E^{1/2}ft} \right),$$

where  $E = K/2fH^2$  is the Ekman number,  $x$  is the cross-front coordinate, and other notation is

---

\* The National Center for Atmospheric Research is sponsored by the National Science Foundation.

---

*Corresponding author address:* Dr. C. Snyder, NCAR, P.O. Box 3000, Boulder, CO 80307-3000. e-mail: *chriss@ucar.edu*

conventional. Thus, the baroclinic zone weakens with time, and surface stress is frontolytical.

Frontolysis occurs because Ekman pumping spins down the interior flow, *not* because diffusion acts directly to smooth the front. In fact, in the Ekman layer frontogenetical and frontolytical effects balance to leading order; for example, stretching of planetary vorticity balances the vertical diffusion of relative vorticity.

If the cross-frontal scale is small and gradients are large [specifically, when  $v_x = O(f)$ ], advection within the PBL becomes important and the effect of the PBL becomes frontogenetic. Heuristically, the front is associated with positive relative vertical vorticity; hence, the flow within the PBL is typically convergent at the front, enhancing surface frontogenesis.

This effect is evident in nonhydrostatic numerical simulations of either an initially geostrophic front subjected to surface drag or of a growing 2D Eady wave. The simulations of frontal spin-down treat the same physical problem as the quasi-geostrophic solution above, except that the evolution of the PBL flow is explicitly calculated and the initial front is sufficiently narrow ( $v_x = 2.5f$ ) that quasi-geostrophy is inaccurate. [See Dunst and Rhodin (1990) for similar simulations.] Surface drag is based on a roughness length of 0.5 m, and  $K$  is

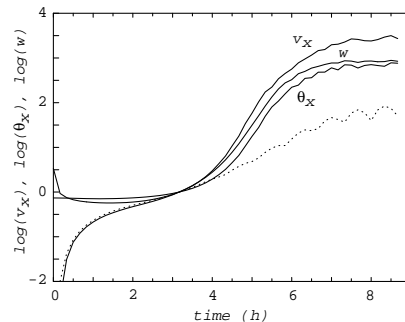


Figure 1. Time series of logarithms of the maximum  $v_x$  and  $\theta_x$  at the lowest model grid level ( $z = 28$  m), and of the maximum  $w$ , from the frontal spin-down calculation. Each quantity is normalized by its value at  $t = 3$  h; for reference, at  $t = 9$  h, the maximum  $v_x$ ,  $\theta_x$  and  $w$  are  $50 \times 10^{-4} \text{ s}^{-1}$ ,  $1.6 \text{ K km}^{-1}$  and  $2.1 \text{ m s}^{-1}$ , respectively. The dotted line shows the maximum  $w$  from a simulation with horizontal resolution reduced by a factor of 8, illustrating how the frontogenesis is limited by resolution.

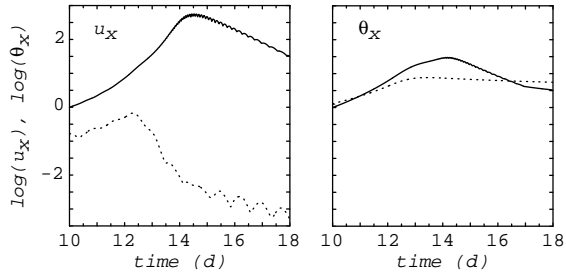


Figure 2. Time series of logarithms of the maximum  $u_x$  and  $\theta_x$  from the Eady wave simulation at levels 550 m above the surface (solid) and below the lid (dotted). Each quantity is normalized by its value at day 10 at 550 m above the surface.

given by the scheme of Troen and Mahrt (1986), which estimates a PBL depth and a local profile for  $K$ . The simulations discussed here use vertical grid spacing  $dz = 56$  m and horizontal grid spacing  $dx = 390$  m.

Figure 1 shows time series of the maximum surface  $v_x$  and  $\theta_x$  and of the maximum  $w$ . Following an initial 2–3 h period of adjustment to the surface drag and mixing, frontogenesis begins and continues at a faster-than-exponential rate until the frontal gradients reach the grid scale.

The frontogenesis is robust with respect to the numerical details of the simulation. It depends only weakly on the parameterization of  $K$ ; even the use of constant  $K = 5 \text{ m}^2 \text{ s}^{-1}$  delays the contraction of gradients to the grid scale by only an hour. Similar frontogenesis also occurs if the model initial conditions are varied. For example, initializing with subgeostrophic low-level winds enhances frontogenesis during the first 2–3 h, but thereafter frontogenesis continues at similar rate to that shown in Fig. 1. This robust behavior, coupled with the fact that after the grid scale is reached the frontal gradients remain nearly constant through 24 h (not shown), indicates that the frontogenesis is frictionally driven and is not produced by inertial oscillations associated with the impulsive imposition of surface drag.

The simulation of the 2D Eady wave, which uses a constant  $K = 10 \text{ m}^2 \text{ s}^{-1}$  and a basic state with  $\bar{\theta}_y = 9.2 \text{ K} (10^3 \text{ km})^{-1}$ , has two novel features designed to highlight the contribution of the PBL to surface frontogenesis. First, thermal-wind balance is enforced at the rigid upper boundary, so that a viscous boundary layer is not required there. Second, the basic-state  $\bar{\theta}_y$  and  $\bar{u}_z$  are assumed to decay, beginning at day 12, as  $\exp[-(t - t_c)^2 / \sigma^2]$ , where  $t_c = 12$  d and  $\sigma = 1$  d. This reduces geostrophic frontogenesis by 90% by day 13.5. Grid spacings in this simulation are  $dz = 100$  m and  $dx = 8$  km.

Figure 2 shows time series of maximum  $u_x$  and  $\theta_x$  at levels 550 m above the surface and below the lid. These time series clearly indicate that, in contrast to the nearly inviscid frontogenesis at the lid, frictionally driven flow in the PBL contributes significantly to the surface frontogenesis: (1) Although  $u_x$  near the lid decays rapidly as the geostrophic forcing decays, the low-level convergence continues to increase. (2) Frontogenesis near the lid ceases by 13 d, while the low-level  $\theta_x$  increases between 13 d and 14 d at half its former rate.

### 3. THE SURFACE FRONT

Because surface drag is strongly frontogenetic for mesoscale fronts, surface fronts will frequently be very narrow (as evidenced, for example, by the common “narrow cold frontal rainband”). In the limit of small  $l$ , where  $l$  is the cross-front scale, the cross-front acceleration and pressure gradient will balance, since these are the only terms in the cross-front momentum equation that scale as  $l^{-1}$ . A density current exhibits the same balance, and thus a narrow surface front is likely to have similarities to density currents. Here, we show that simulations of sufficiently high resolution do produce this balance, and we offer preliminary thoughts on the relation of the surface front to a density current.

Velocities and  $\theta$  from the simulation of frontal spin-down are displayed at  $t = 7$  h in Fig. 3. The PBL flow has advected the cold air forward (i.e., toward warmer air) at low levels, resulting in a

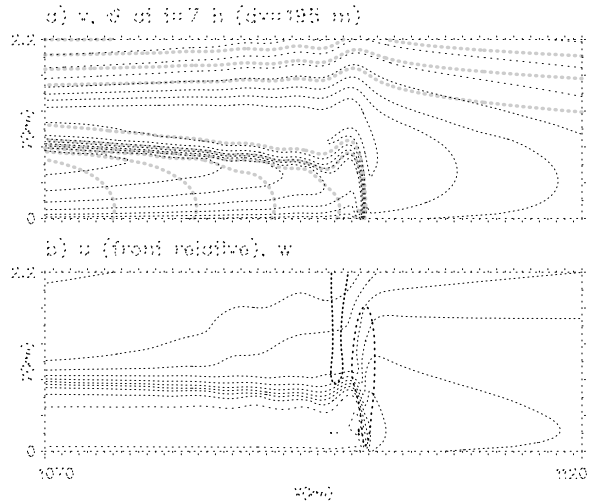


Figure 3. The spin-down simulation at 7 h: (a)  $v$  (contour interval  $1 \text{ m s}^{-1}$ ) and  $\theta$  (heavy stippled lines, contour interval  $0.5 \text{ K}$ ); (b)  $u$  relative to the frontal speed of  $5.5 \text{ m s}^{-1}$  (contour interval  $1 \text{ m s}^{-1}$ ), and  $w$  (bold lines, contours at  $\pm 0.5 \text{ m s}^{-1}$ ). Only 50 km, and the lowest 2.2 km, of the computational domain ( $1350 \text{ km} \times 9 \text{ km}$ ) is shown. Spacings of tick marks on the vertical and horizontal axes are, respectively, 225 m and 780 m, or 4 grid intervals.

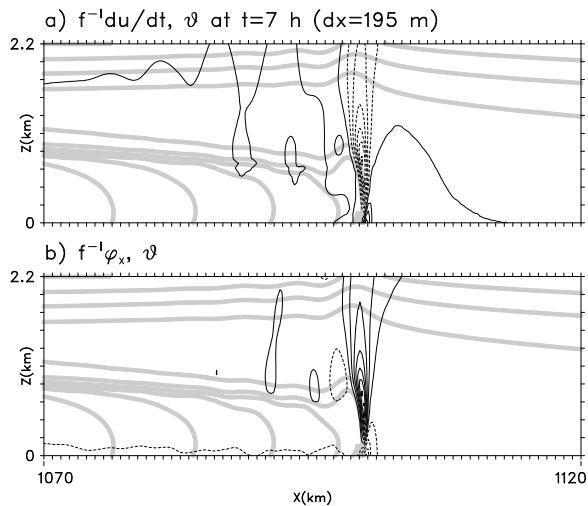


Figure 4. As in Fig. 3, but showing: (a)  $f^{-1}du/dt$  and (b)  $f^{-1}\phi_x$  (both, contour interval  $30 \text{ m s}^{-1}$ ) overlaid on  $\theta$ .

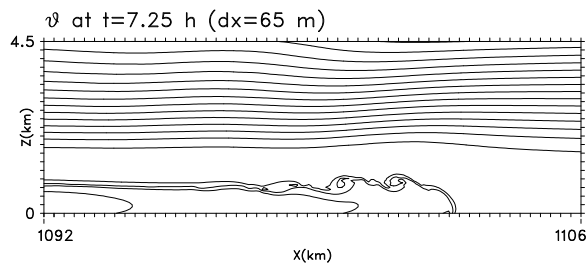


Figure 5. Potential temperature,  $\theta$ , from spin-down simulation at 7.25 h, using  $dx = 65 \text{ m}$ . The domain shown differs from that of Figs. 3 and 4, and is plotted with aspect ratio 1:1. Tick marks again correspond to 4 grid intervals.

sharp inversion above the cold air as discussed in Keyser and Anthes (1982). By this time, the leading edge of the surface front is exceedingly sharp, with the strongest gradients concentrated in a few grid intervals (less than 1 km).

The updraft at the leading edge has maximum velocity over  $1 \text{ m s}^{-1}$ , even though the simulation ignores moist processes. Since the atmosphere is stably stratified, the frontal passage produces vertically propagating gravity waves, much as flow over a ridge. Thus, subsidence of similar magnitude follows the updraft, and ripples are evident in the isentropes in the stably stratified layers.

Interestingly,  $\theta$  decreases by only 0.5 K across the leading edge of the front. Frontal passage is accompanied instead by an abrupt wind shift and the onset of a steady decrease in temperature.

Figure 4 depicts the cross-front acceleration and pressure gradient. These terms balance near

the leading edge of the front, as predicted by the scaling argument and as is characteristic of a density current. Away from the leading edge, however,  $du/dt$  is small, so that the balance of forces within the PBL is as in the Ekman layer and differs fundamentally from that in a density current.

If the horizontal resolution is increased, additional fine structure appears in the solutions. Figure 5 shows  $\theta$  from a simulation with  $dx = 65 \text{ m}$ . (Because of computational limitations, this simulation was initialized at 6 h on a reduced horizontal domain of 170 km, using the solution with  $dx = 195 \text{ m}$ .) The leading edge of the front again contracts to the grid scale, and Kelvin–Helmholtz billows now appear on the inversion. The qualitative resemblance to a laboratory density current is unmistakable.

The degree to which the dynamics of the flow shown in Fig. 5 are similar to those of a density current, however, is not clear. Ignoring rotation, turbulent stress divergence, and gradients of  $\theta$  in the cold air, and treating the top of the weakly stratified layer (at  $z = 1.75 \text{ km}$ ) as a rigid lid, the density current propagation speed is  $c = F(gh\Delta\theta/\theta_0)^{1/2}$ , where  $h$  and  $\Delta\theta$  are, respectively, the depth and potential temperature deficit of the cold air. Taking  $\Delta\theta$  to be 0.5–1.5 K, and using  $F = 1/\sqrt{2}$  (based on a ratio of 1/2 of the depth of the cold air to the depth of the weakly stratified layer; Benjamin 1968) gives  $c = 2.7\text{--}4.7 \text{ m s}^{-1}$ . If density current dynamics govern the frontal propagation, then  $c$  should equal the front-relative speed of the oncoming warm air, which is  $3\text{--}4 \text{ m s}^{-1}$  (Fig. 3b). Clearly, the two are comparable, but one must ask why rotation, stress divergence, etc. should be negligible. We are currently attempting to understand how the local dynamics of the frontal nose, which are dominated by the balance between cross-front acceleration and pressure gradient, match to the mesoscale dynamics of the front and the PBL, in which rotation and turbulent stresses restrain the flow from accelerating down the pressure gradient.

*Acknowledgments.* DK was supported by NSF Grant ATM-9421678 awarded to SUNY/Albany.

## REFERENCES

- Benjamin, T. B., 1968. *J. Fluid Mech.*, **31**, 209–248.
- Dunst, M., and A. Rhodin, 1990. *Contr. Atmos. Phys.*, **63**, 223–242.
- Keyser, D., and R. A. Anthes, 1982. *J. Atmos. Sci.*, **39**, 1783–1802.
- Troen, I. B., and L. Mahrt, 1986. *Bound.-Layer Meteor.*, **37**, 129–148.